ORBITAL DEBRIS SIZE ESTIMATION FROM RADAR CROSS SECTION MEASUREMENTS

N. Rajan[(1)], T. Morgan[(2)], R. Lambour[(3)], I. Kupiec[(4)]
[(1)-(4)]MIT Lincoln Laboratory, 244 Wood St. Lexington, MA 02420-9185
rajan@ll.mit.edu, morgan@ll.mit.edu, lambour@ll.mit.edu, kupiec@ll.mit.edu

ABSTRACT

MIT Lincoln Laboratory has conducted a measurement program for man-made orbital debris since 1991 in response to NASA's need to characterize the orbital debris population and facilitate manned spaceflight activities. The primary sensors used in that effort are the Haystack and Haystack Auxiliary (HAX) radars located at the Lincoln Space Surveillance Complex (LSSC) in Westford, Massachusetts. This paper will describe the first year results from a new effort being conducted at LSSC, the objective of which is to assess NASA's current procedure for the determination of debris size from RCS data. RCS data will be acquired from NASA-selected 43 Resident Space Objects (RSO). Results will be compared to the size estimates from the FPS-85 radar, an asset of the Space Surveillance Network.

1. INTRODUCTION

The number of orbital debris fragments in the size range of 1-30 cm has been estimated at over 100,000. This is a fairly large number and raises concerns regarding the safety of satellites in orbit and their ability to withstand impacts from orbital debris. Characterization of the orbital debris environment is relevant to the deployment of all man-made objects in space. In addition, the debris fragments represent potential radar and optical clutter for ground-based and space-based surveillance systems.

In order to quantify the risk posed to satellites by the orbital debris population, NASA has undertaken a statistical characterization of the orbital debris environment. MIT Lincoln Laboratory has participated in this effort since 1991 with the Haystack and Haystack Auxiliary (HAX) radars located at the Lincoln Space Surveillance Complex (LSSC) in Westford, Massachusetts. These radars have been utilized in a staring mode to collect data on the near-Earth orbital debris population [1]. In addition, the FPS-85 space surveillance radar located at Eglin AFB, Florida, has also contributed a significant amount of data on near-Earth orbital debris obtained during its normal operation.

These data sources have allowed NASA to characterize the population of orbital debris. The number of debris fragments and their distribution as a function of altitude and inclination has been estimated and has allowed the development of orbital debris environment models which are used to specify the environment for objects such as the International Space Station. Also of importance is knowledge of the size distribution of the debris fragments. When discussing size, we refer to an equivalent sphere diameter (ESD), which is the inferred diameter of an object calculated under the assumption that it is spherically shaped. If the size of an object is known, an estimate of its mass, and thus impact energy, can be made. Knowledge of impact energy facilitates determination of satellite vulnerability. In addition, the effects of atmospheric drag on the object can be estimated and, thus, its orbital lifetime. This allows introduction of a time-dependent component into the modeling of the orbital debris environment.

The size of the object must usually be estimated from radar cross-section (RCS) data. NASA has developed an RCS-to-ESD mapping function, which is referred to as the Size Estimation Model (SEM) [2]. This model was derived from multi-frequency radar range data collected on ~40 simulated orbital debris fragments produced by a hypervelocity collision. The pieces were observed at a number of different frequencies and orientations and RCS probability density functions were derived to characterize the RCS as a function of frequency and object size. The end result is presented in Fig. 1, which shows a graph of RCS normalized to the square of the wavelength as a function of ESD normalized to wavelength. The data from the ~40 fragments are shown as points and the mapping function is shown as a solid line overlaying the data. The ESD of debris objects is routinely estimated by using this RCS-to-ESD mapping function with the FPS-85 data; this has

Proceedings of the 3rd European Conference on Space Debris, ESOC, Darmstadt, Germany, 19 - 21 March 2001
(ESA SP-473, August 2001)

produced a catalog of size estimates for debris objects.

NASA has begun using the Liquid Mirror Telescope located in Cloudcroft, New Mexico, to acquire additional debris observations. This is a zenith-staring, 3-m aperture telescope that was built to characterize the optical orbital debris environment in the 1-10 cm size range [3]. Diameters for debris objects can be derived from the optical data once an optical phase function and albedo are either determined or assumed for the objects. NASA recently compared these optical diameters and the radar diameters from the FPS-85 data and noted some discrepancies. Those discrepancies have led to a new program to characterize a number of debris objects and gain insight on the RCS-to-size estimation procedure. This study is separate from the ongoing debris observation program at LSSC using the Haystack and HAX radars. This paper will provide an overview of our objectives and techniques, present results from the first year of the program, and describe ongoing program effort at LSSC.

2. OBJECTIVES AND APPROACH

The objective of the current program is to gain insight on the procedure for the determination of size from RCS. NASA has selected a set of 43 relatively small RSOs for characterization (cf., Table 1) by the three radars at the LSSC. The radars are shown in Fig. 2. At the end of the first phase of the program (October 1999), data collection had been completed on 16 of the 43 objects. Those 16 objects are highlighted in Table 1. Data collection is underway on the remaining 27 objects.

During the first phase of the program, each RSO was tracked jointly by the Millstone and Haystack radars and also by the Millstone and HAX radars. Each RSO was tracked at three different elevation angles in order to provide a wide range of aspect angles. Every attempt was made to duplicate the pass geometries for each pair of radars, but this proved difficult in practice. The end result is 6 joint tracks for each object. The data for RCS and size characterization were collected using narrowband waveforms with the Millstone, Haystack and HAX radars. During each track, Haystack and HAX also collected short segments of wideband data, which can be used to provide an independent size estimate, if necessary. In addition, radar calibration spheres were tracked whenever possible during the debris tracking sessions in order to provide data on the radar calibration.

All three radars recorded RCS vs. time in the principal polarization (PP) and orthogonal polarization (OP) channels. The RCS data were integrated non-coherently over a time span of approximately 200 msec. For Haystack, this integrated measurement is equivalent to the type of data collected by the radar when it is operating in staring mode for debris data collection. These integrated RCS measurements are sent through the NASA SEM in order to derive the equivalent sphere diameter (ESD) at ~200 msec intervals. Fig. 3 presents a flowchart that describes the size estimation procedure. The RCS data are integrated and the PP and OP returns are summed (PP+OP). The summed measurements are normalized by the square of the wavelength and the corresponding value of d/λ is interpolated from the NASA SEM curve. For any given track, this procedure produces a time series of ESDs. These size estimates are then examined statistically in order to derive a representative size for the object. The statistical quantities calculated for each track of an object are listed in Table 2. The mean size represents an average size for the object over the course of the track. Histograms of the PP and OP RCS, the PP/OP ratio, and the ESD estimates are also generated.

Examination of the ESD histograms shows that multiple peaks often characterize the size distribution for an object. An example of this behavior is shown in Figure 4. Peaks are evident in the size distribution at ~6, ~11, and ~20 cm. This presence of multiple peaks in the size distribution suggests that the radar observed more than one characteristic dimension for the object. These observations have led us to attempt to derive two representative sizes for each object. These sizes are intended to represent a long and a short dimension for the object. We have termed this analysis a clustered statistical analysis.

For each object, a cumulative distribution function (CDF) and a probability density function (PDF) are calculated using all of the data collected. This calculation is done separately for each radar. The size corresponding to the 75% point is selected as the threshold size at which to separate the size distribution into two. The PDF is examined to ensure that this 75% size is a reasonable point at which to separate the data. Then, a mean, standard deviation, and median size is calculated from the two separated size distributions. These statistics represent two characteristic sizes for the object, a short and long dimension. The narrowband RCS signature sometimes also allows us to perform an independent assessment of the size of the object using theoretical

arguments. An example of this type of analysis will be presented in the next section.

As a last step, an object folder is generated for each object, summarizing the track histories, RCS data and size estimates as well as their associated statistics, cluster analysis, and narrowband signature analysis.

3. RESULTS

We now present an example of the data collected and the results of the statistical analysis. We consider Object 4719, which is debris from the breakup of an Agena D upper stage that took place in 1970. No *a priori* knowledge of the size of the object other than the size estimate generated from the FPS-85 radar is available. That size estimate is 0.86 meters and represents an ESD.

The Millstone Hill radar (MHR) data on this object show a repeatable specular lobing pattern in the PP return for all tracks collected. An example is shown in Fig. 5. This pattern facilitates size estimation from the narrowband signature. The peak-to-peak period in the PP data is ~20-25 seconds. The right hand side of Figure 6 presents an expanded view of several of the specular peaks. RCS lobing features suggest that we are looking at an object that has one dimension significantly longer than the other, like a thin cylinder or dipole-shaped object. The specular returns in the PP channel are then the reflection from the cylinder when it is viewed broadside, and the lower-amplitude, wider returns in the same channel would be the reflection from the smaller ends of the object. It is assumed that the object is tumbling. Using the end-over-end motion assumption and assuming that the object is shaped like a cylinder, we can estimate the dimensions of the object using the specular peaks. The tumble rate is 2π in ~50 sec or 0.126 rad/sec. The null-to-null width of the main lobes of the specular reflections is ~1 sec. Using $\theta=\lambda/L$, this suggests a long dimension of ~1.84 m. Then, the amplitude of the specular (~8 dBsm) can be used to estimate the second dimension from $RCS = kaL^2$. The second dimension, a, is about 7 cm. Repeating this analysis with a number of different specular peaks suggests that the object is long and thin, with a short dimension of ~10-20 cm and a long dimension of 1.5-2.5 m.

Fig. 6 presents the mean and median size estimates for Object 4719 derived from the LSSC data. There is fairly good agreement in the mean and median sizes derived by the three radars from track to track. However, the mean and median size estimates fall well below the FPS-85 size estimate and the standard deviations are high. The high deviations are due to the observation of specular reflections during the tracks. For the same reason, the means tend to be well above the median values for all of the tracks. These estimates suggest that the object has a mean size of 0.53 – 1.22 m and a median size of 0.28 – 0.70 m. These means and medians have a wide range of values, and are not in good agreement with the size estimates derived from the narrowband signature.

The above analysis suggests that the radars observed an object which is not well characterized by one size estimate. Therefore, a clustered statistical analysis for Object 4719 was performed. The 75% point in the CDF corresponds to a size of 0.733 m for the MHR data, and a size of 0.4275 m for the combined Haystack/HAX data sets. The size distribution for each track was split at the appropriate threshold value and statistics were calculated on the data above and below these points. The results for the LSSC data are shown in Fig. 7. For the MHR data, the mean and median values for the short axis are very consistent from track-to-track and range from 0.16 – 0.29 m. The mean and median values for the long axis are more variable. Mean values range from 1.94 – 4.02 m and median values range from 1.21 – 1.5 m. These results from MHR are consistent with the narrowband signature analysis results described earlier. The results for Haystack and HAX lack the same consistency as the MHR results (they are more variable from track to track) but are roughly consistent with the MHR results. The mean sizes for the short dimension of the object are 0.24-0.6 m and the median values for the short dimension range from 0.23-0.59 m. For the long dimension, the mean sizes are 1.4-2.9 m and the median sizes are 0.8-2.03 m.

In summary, it can be concluded that Object 4719 is a long, thin, roughly cylindrical shaped object with a short dimension of ~10-30 cm and a long dimension of ~1.4 – 3.0 m. The slight discrepancies in estimated sizes for the three radars suggest that Object 4719 is more complex than a simple cylinder.

In Table 3, we present the results of our analysis on the first 16 objects. The table presents the object number, the derived sizes for short and long dimensions from each radar. The FPS-85 derived size is also presented between the short and long dimension size estimates. HAY refers to Haystack. We note that the sizes derived from the LSSC radars are usually consistent with one another and that the consistency between the three radars was improved by performing the clustering analysis. This improvement in consistency was demonstrated for object 4719 in

this paper and is true in general for the 16 objects examined so far. We also note that the short and long dimension size estimates tend to bracket the size estimates from the FPS-85, which suggests that the FPS-85, observed the object at some random aspect angle and that the resulting size estimate lies between the minimum and maximum dimensions of the object. The FPS-85 size estimates result from a single observation as the object penetrated the radar beam at a single orientation. The consistency across frequencies and the bracketing of the FPS-85 size observations suggest that the size estimation technique is producing good results at multiple frequencies.

4. SUMMARY AND CURRENT STATUS

Multi-frequency RCS data have been collected on 16 out of 43 objects selected by NASA for characterization. Each object was tracked jointly by MHR/Haystack and MHR/HAX over three different elevation angles for a total of six tracks per object. The data from each track was analyzed and statistics were generated for the PP and OP RCS, the PP/OP ratio, and the ESD estimates. In addition, a clustered data analysis has been performed on the size estimates for those objects that appear to have more than one characteristic size. The results of these analyses have been collected in object folders. Preliminary characterization of these 16 objects was completed in February 2000. The data collection is ongoing. In addition, further investigation of data clustering techniques continues, since our results vary with the threshold size selected

Table 1. List of Objects Selected for Characterization

Object	FPS-85 Size	Notes B: Breakup, US: Upper stage USB: Upper stage breakup
20	**0.85**	**Vanguard 3**
82	**1.1**	**Scout X-1 US**
85	0.19	Explorer 9 debris
155	**0.23**	**Debris from Able-Star USB**
324	0.16	Debris from Able-Star USB
341	**0.71**	**Delta US**
462	0.21	Debris from Able-Star USB
2121	0.83	OV1-4
4712	0.15	Soviet ASAT debris
4719	**0.86**	**Debris Agena D B**
5187	0.31	Soviet ASAT debris
6350	**1.67**	**Cosmos 546**
7042	0.31	Debris Delta 2nd stage B
7050	0.26	Debris Delta 2nd stageB
7185	0.2	Debris Delta 2nd stage B
8614	**0.97**	**Cosmos 798**
9982	0.26	Tansei-03 debris
10841	0.16	Debris Delta 2nd stage B
12542	**0.43**	**Debris Delta 2nd stage B**
13377	**0.96**	**Cosmos 1390**
13511	0.13	Debris Able-Star USB
14357	**0.2**	**Debris Cosmos 1275 B**
14569	**0.31**	**ETS-3 debris**
15005	**0.97**	**Cosmos 1566**
16268	0.34	Debris Cosmos 1691 B
17023	0.17	Debris Delta 2nd stage B
17478	0.11	Debris Ariane USB
17805	**0.14**	**Debris Cosmos 1375 B**
18361	**1.92**	**Transit 19**
18530	0.18	Oscar 27 debris
18599	0.3	Debris Delta 2nd stage B
21101	**0.99**	**Cosmos 2126**
21114	1.32	SL-12 auxiliary motor
21386	0.14	Debris Delta-1USB
21523	0.16	Debris Delta-1 USB
21835	**1.05**	**Magion 3**
22415	0.39	Debris SL-16 USB
22443	0.15	Debris SL-16 USB
23297	0.25	Cosmos 1710 debris
23486	0.17	Debris SL-19 USB
23952	0.18	Ops 0856 debris
24124	0.21	Debris from Pegasus HAPS breakup

5. REFERENCES

1. Setteceri, T. J., et al., *Haystack Radar Measurements of the Orbital Debris Environment; 1994-1996*, JSC-27842, NASA Johnson Spaceflight Center, Houston, TX, May 1997.

2. Bohannon, G. E., and N. Young, *Debris Size Estimation Using Average RCS Measurements*, Report No. 930781-BE-2247, XonTech, Inc., Los Angeles, CA, September 1993.

3. Africano, J. L., et al., *NASA/JSC Optical Orbital Debris Program: Results from the Liquid Mirror Telescope (LMT) and the CCD Debris Telescope (CDT)*, in Proceedings of the 1999 Space Control Conference, Project Report STK-254, MIT Lincoln Laboratory, Lexington, MA, April 1999.

4. Caprara, G., *The Complete Encyclopedia of Space Satellites*, Portland House, New York, NY, 1986.

Table 2. Statistical Quantities Tabulated During Object Characterization

Minimum and Maximum PP and OP RCS values
Mean and Standard Deviation of PP and OP RCS, PP/OP ratio, and ESD estimates
Median of PP and OP RCS, PP/OP ratio, and ESD estimates
Mean Absolute Deviation of PP and OP RCS, PP/OP ratio, and ESD estimates
5% and 95% values for PP and OP RCS, PP/OP ratio, and ESD estimates

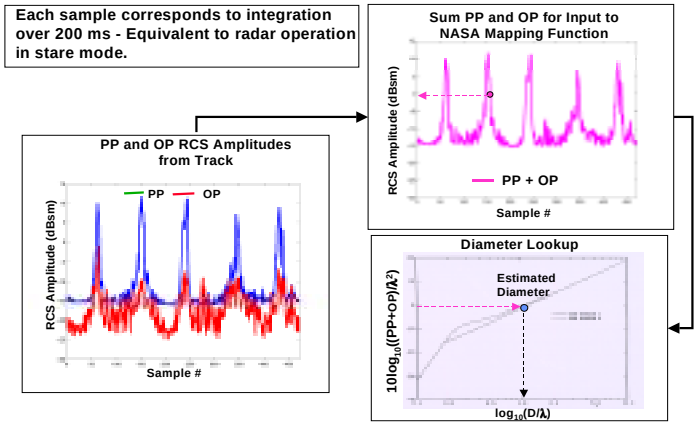

Figure 3. Flowchart describing the size estimation procedure.

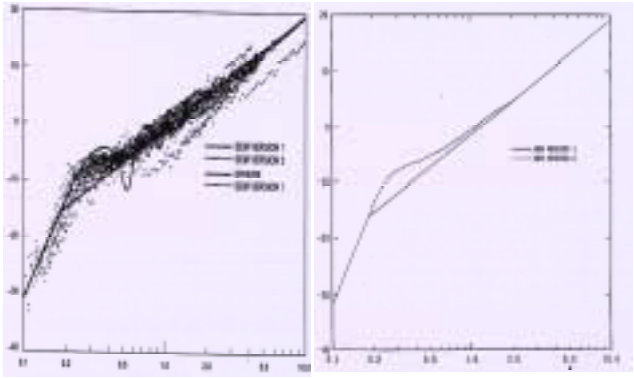

Figure 1. (Left) The RCS data used to derive the NASA SEM Version 2. The overlaid curve represents the RCS of a sphere. The x-axis for both plots is diameter/λ and the y-axis is RCS/λ^2; (Right) The NASA SEM curve derived from the RCS measurements. The dashed curve labeled version 2 is the mapping function used in this paper.

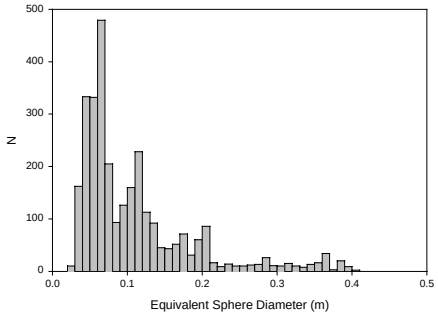

Figure 4. Distribution of ESD estimates for object 14357. The data used to produce the size estimates were collected on day 216 of 1999 with the Millstone Hill Radar.

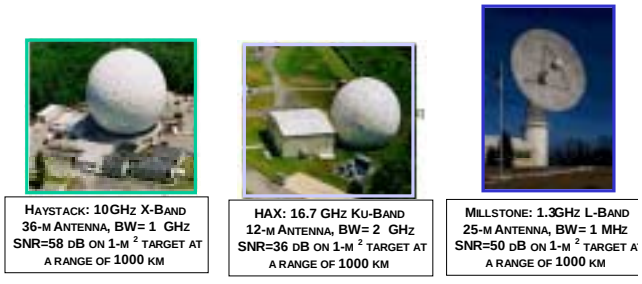

Figure 2. Radars located at Lincoln Space Surveillance Complex in Westford, Massachusetts.

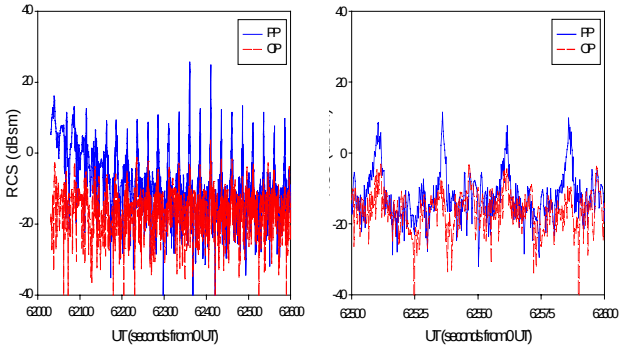

Figure 6. (Left)PP and OP RCS data on Object 4719 obtained at MHR on day 146, 1999; (Right) The same data set expanded to shown detail.

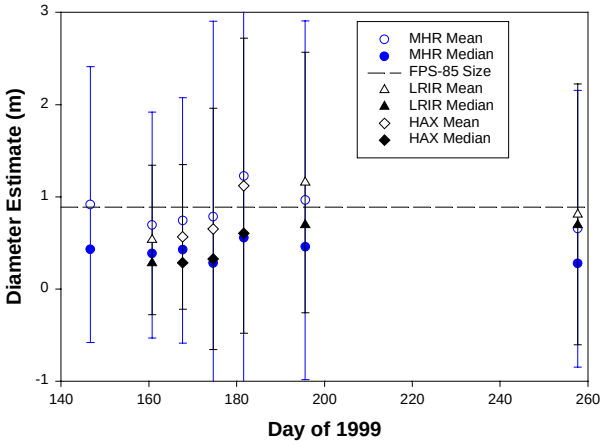

Figure 6. Mean and Median size estimates for Object 4719 from Millstone (MHR), Haystack (LRIR), and HAX. The FPS-85 derived size estimate is plotted as a dashed line for reference.

Table 3. Estimated Sizes for Debris Objects
M: MHR, HY: Haystack, HX: Haystack Auxilliary
Sh: Short Axis, Lg: Long Axis

Obj #	M Sh	HY Sh	HX Sh	FPS Size	M Lg	HY Lg	HX Lg
20	0.47	1.03	0.78	0.85	1.01	1.82	1.86
82	0.42	0.62	0.63	1.10	0.91	1.33	1.39
155	0.08	0.12	0.12	0.23	0.18	0.15	0.16
341	0.34	0.69	-	0.71	0.87	1.33	-
4719	0.29	0.28	0.32	0.86	1.47	0.74	1.00
6350	0.90	1.65	2.06	1.67	2.02	4.14	5.57
8614	0.63	0.65	0.69	0.97	1.05	1.61	1.38
12542	0.06	0.09	0.38	0.43	0.29	0.31	0.52
13377	0.74	0.59	0.60	0.96	1.21	1.41	1.33
14357	0.05	0.09	0.14	0.20	0.18	0.31	0.33
14569	0.09	0.11	0.13	0.31	0.18	0.17	0.16
15005	0.68	0.57	0.59	0.97	1.15	1.59	1.64
17805	0.06	0.09	0.19	0.14	0.16	0.32	0.52
18361	0.64	0.94	0.99	1.92	1.56	1.72	1.81
21101	0.63	0.42	0.57	0.99	1.13	1.18	1.21
21835	0.55	0.67	0.75	1.05	1.21	1.21	1.63

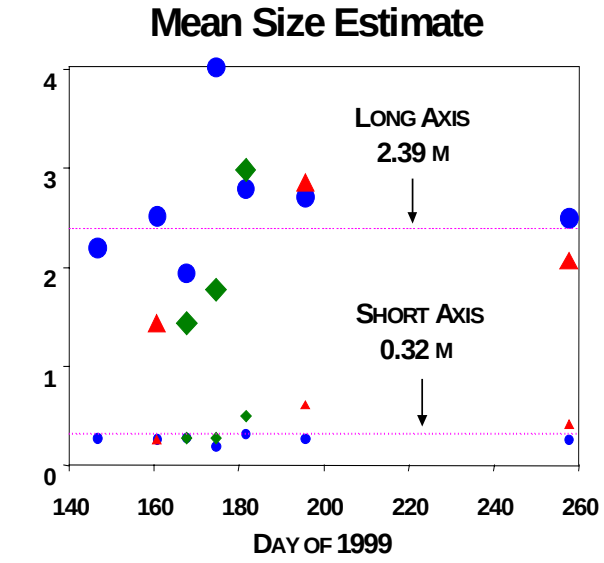

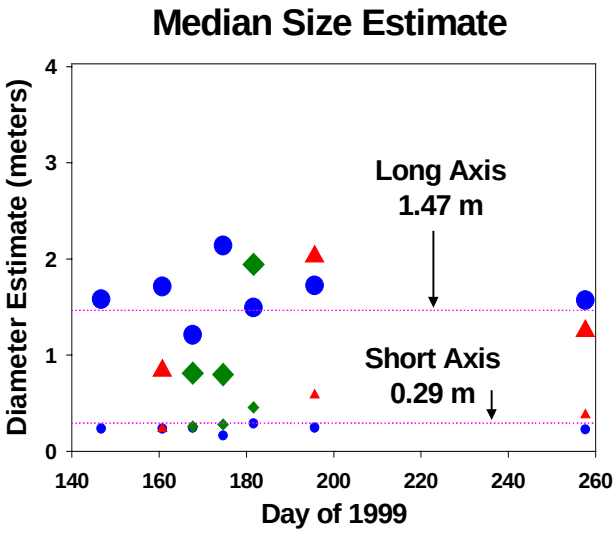

Figure 7. Mean (top) and median (bottom) size estimates from LSSC data for the short (small symbols) and long (large symbols) dimensions of Object 4719. MHR data are represented by circles, Haystack data by triangles, and HAX data by diamonds.